Food Chemistry: X 14 (2022) 100274

Contents lists available at ScienceDirect

Food Chemistry: X

journal homepage: www.sciencedirect.com/journal/food-chemistry-x

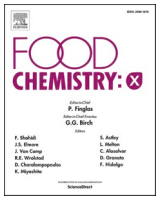

Effect of γ-irradiation on structure, physicochemical property and bioactivity of soluble dietary fiber in navel orange peel

Xiaoni Li [a,1], Biying Wang [b,1], Wanjun Hu [a], Haiguang Chen [a], Zhili Sheng [c], Bao Yang [c,*], Limei Yu [a,*]

[a] College of Light Industry and Food Sciences, Zhongkai University of Agriculture and Engineering, Guangzhou 510225, China
[b] College of Food Sciences, South China Agricultural University, Guangzhou 510640, China
[c] Guangdong Provincial Key Laboratory of Applied Botany, South China Botanical Garden, Chinese Academy of Sciences, Guangzhou 510650, China

ARTICLE INFO

Keywords:
Dietary fiber
Polysaccharide
Molecular weight
Structure
Pectin

ABSTRACT

Soluble dietary fibers are widely used in functional food. In this work, the effects of γ-irradiation on molecular weight, structure, physicochemical properties and bioactivities of soluble dietary fiber in navel orange peel (OSDF) were investigated. Γ-irradiation enhanced the extraction yield of OSDF. The molar ratio of glucose and galacturonic acid was increased. The molecular weight profile of OSDF was modified. Γ-irradiation (3–6 kGy) improved the water holding capacity, water swelling capacity, oil holding capacity, cation-exchange capacity, nitrite adsorption capacity and total antioxidant capacity of OSDF. Glucose adsorption capacity and bifidobacterium proliferation capacity of OSDF were improved in a dose-dependent behaviour. Moreover, γ-irradiation promoted the cracking of microstructure. FT-IR spectra showed that more carboxyl groups were newly formed by γ-irradiation. These findings indicated that γ-irradiation treatment was an efficient technique for improving physicochemical properties and health benefits.

Introduction

Navel orange (*Citrus sinensis Osbeck*), a famous sweet orange variety, belongs to the *Citrus* genus of *Rutaceae* family. It is widely cultivated around the world. Ganzhou city is the largest production area of navel oranges in China with the planting area of 103,200 ha and the annual production of 1.2 million tons. The peel of navel orange is a good resource of dietary fiber, which accounts for about 30% of the whole fruit weight. Dietary fiber is described as a group of carbohydrate polymers or oligomers that escape digestion in the small intestine, and partially or completely fermented in the large intestine by gut microbiota (Fuller, Tapsell, & Beck, 2018). It can improve intestinal immune function and has a potential health benefit in maintaining gut microecological equilibrium (Huang, Zhao, Mao, Chen, & Yang, 2021; Gill et al., 2021), lowering blood lipids, stabilizing blood glucose levels (Shridhar et al., 2018), and decreasing incidences of several diseases (Threapleton et al., 2013). Based on the solubility, dietary fibers are divided into insoluble dietary fiber and soluble dietary fiber. The main advantage of dietary fiber from orange peel, compared with other sources, is its high proportion of soluble dietary fiber. Previous study showed that soluble dietary fiber could balance dietary fiber intake and replenish the essential nutrient element of the human body, which has attracted the attention of researchers (Sang et al., 2021). Compared with the insoluble dietary fiber, orange soluble dietary fiber (OSDF) presented better functional properties, such as fermentability, solubility, and water/oil holding capacity (Chen et al., 2020).

The nutritional value and functional characteristics of dietary fiber are influenced by chemical composition and structure (Yang, Gao, & Yang, 2020). Several techniques have been applied to modify dietary fiber. Extrusion, acidic hydrolysis, enzymatic hydrolysis, microbial fermentation and ultrasound treatment can improve the functions. Wen et al. (2017) have found that enzymatic modification for rice bran dietary fiber can enhance the soluble dietary fiber content and improve the cholesterol absorption capacity. Steam explosion can increase the content of soluble polysaccharides by breaking the glycosidic and hydrogen bonds from cellulose and hemicellulose. Microbial fermentation can improve water holding capacity, water swelling capacity, and anti-diabetic effect (Min et al., 2018).

* Corresponding authors.
E-mail addresses: yangbao@scbg.ac.cn (B. Yang), biyingwang2003@163.com (L. Yu).
[1] Both authors contribute equally to this paper.

https://doi.org/10.1016/j.fochx.2022.100274
Received 17 January 2022; Received in revised form 23 February 2022; Accepted 24 February 2022
Available online 25 February 2022

Gamma irradiation is receiving much attention for its effectiveness and technical usefulness in producing degraded products as the process is free of chemical initiators and hazardous side products. Γ-irradiation is considered as an effective physical technique to modify polysaccharides by cross-linking, grafting and degradation (Choi & Kim, 2013). It has been reported that high-dose irradiation can break the structure of lignocellulose and increase the efficiency of enzymatic hydrolysis to increase the dissolution of water-soluble carbohydrates (Li et al., 2020). However, there are also some disadvantages. For instance, high-dose radiation can lead to chemical changes in food products and affect the food's sensory properties, which can produce unpleasant off-flavor and change in color. Besides, radiation could lead to the reduction of some water- and fat-soluble vitamins and the creation of oxidation compounds such as aldehydes, ketones, and alcohols.

To extend the application of dietary fiber in functional food and explore the influence of irradiation intervention on dietary fiber, in this study, navel orange peels were treated at four irradiation doses (3–12 kGy). The structural characteristics were investigated by scanning electron microscopy, X-ray diffraction spectrometry, and infrared spectroscopy. The monosaccharide composition, molecular weight, physicochemical and functional properties were evaluated. These results can provide useful information for the extensively industrial application of navel orange peel.

Materials and methods

Materials and reagents

Fresh navel orange was purchased from Carrefour Supermarket (Guangzhou, China). TPY liquid medium, TPY agar medium, 95% ethanol, sodium hydroxide, and glucose, mannose, rhamnose, galacturonic acid, galactose, and neutral protease were obtained from Borui sugar Biotechnology Co., Ltd. (Shenzhen, China). The other reagents used in the present work were of analytical grade.

Sample preparation

The peel of navel orange fruit was separated and dried at 50 °C in an oven (DHG-9033BS-III, Shanghai Xinmiao Medical Devices Manufacturing Co., Ltd., Shanghai, China) until the water content was below 10%. The dried samples were crushed by a high-speed pulverizer (Ruian, Yonglu Pharmaceutical Co., LTD, Zhejiang, China) and passed through a 60-mesh screen. The sieved powders were irradiated at 0, 3, 6, 9, and 12 kGy by ^{60}Co γ-ray irradiation at 10 kGy doses (Furui High Energy Technology Co., Ltd, Guangzhou, China). The dosimetry was carried out using alanine dosimeters (Bruker Instruments, Rheinstetten, Germany) measured with a Bruker EMS 104 EPR Analyzer. After irradiation, the samples were stored in sealed polyethylene bags at room temperature.

Preparation of OSDF

The OSDF was extracted according to the literature (Rouhou et al., 2018). One gram of navel orange peel powder was dispersed in 20 mL of distilled water, then neutral protease was added (250 U/g) and incubated at 55 °C for 4 h. The mixture was heated in boiling water for 15 min to inactivate the enzymes. After centrifuging at 8000 rpm for 20 min. The supernatant was concentrated by a rotary evaporator (RE-52C; Shanghai Yarong biochemical instrument factory, Shanghai, China) at 60 °C. Afterward, 95% ethanol was added to the concentrated supernatant, standing for 12 h at 4 °C, followed by centrifuged for 15 min at 5000 rpm at room temperature. The precipitates were washed and centrifuged twice with 95% ethanol, then the precipitates were dried at 60 °C for 48 h to obtain OSDF. Dried OSDF were milled using a grinder (Ruian, Yonglu Pharmaceutical Co., LTD, Zhejiang, China) to pass through a 60-mesh sieve, and were stored in aluminum foil at 4 °C for further analysis.

Monosaccharide composition analysis

Monosaccharide composition was measured according to the literature (Sheng, Liu, & Yang, 2021). The OSDF (10 mg) were hydrolyzed in sealed glass tubes containing 10 mL of 3 M trifluoroacetic acid at 120 °C for 3 h in a DHG-9425A cabinet dryer (Shanghai Yiheng Scientific Instrument Co., Ltd., Shanghai, China). The hydrolysates and monosaccharide standards were mixed with hydroxylamine hydrochloride (10 mg) and 1 mL of pyridine at 90 °C for 0.5 h. After adding 1 mL of acetic anhydride, the mixture was incubated at 90 °C for another 0.5 h. Subsequently, the solution was filtered with the 0.45-μm membrane and the final products were determined on an anion chromatography (ICS5000, ThermoFisher) equipped with a DionexCarbopac TMPA20 chromatographic column (3 × 150 mm), an electrochemical detector (30 °C), the flow rate (0.3 mL/min) and the mobile phase (A: H_2O; B: 250 mM NaOH; C: 50 mM NaOH in 500 mM NaOAc).

Molecular weight determination

Gel permeation chromatography (GPC) was carried out to determine the molecular weight of OSDF according to the protocol of Yang et al. (2019). GPC was implemented using a Shimadzu LC-20 A liquid chromatography instrument (Shimadzu Corporation, Kyoto, Japan) equipped with three tandemly linked G6000PWXL, G5000PWXL, and G3000PWXL columns (Tosoh Bioscience, Stuttgart, Germany). OSDFs were dissolved in deionized water and passed through a syringe filter (0.22 μm). A refractive index detector was used for monitoring. The mobile phase was 20 mM phosphate buffer (pH 7.0) at a flow rate of 0.5 mL/min. Dextran standards with different molecular weights (5220, 11,600, 48,600, 147,600, 409,800, 667,800, 2,990,000 kDa) were applied for making the calibration curve. The molecular weight was calculated by retention time.

Determination of physicochemical properties

Water holding capacity

The water holding capacity of OSDF from navel orange peel was determined according to the method described by Gómez-Ordóñez, Jiménez-Escrig, and Rupérez (2000). One gram of OSDF sample (M_d) was mixed with 300 mL of distilled water, followed by one hour of equilibration at 37 °C. After centrifugation at 5000 rpm for 10 min, the residues were collected and weighed (M_w). Water holding capacity was calculated as follows:

$$\text{Water holding capacity (g/g)} = (M_w - M_d) / M_d$$

where M_w is the wet weight of the sample (g), and M_d is the dry weight of the sample (g)

Oil-holding capacity

Five grams of OSDF sample was mixed with 200 mL of corn oil (Shandong Luhua Group Co., Ltd., Shandong, China) at 37 °C for 2 h, and then the mixture was centrifuged at 5000 rpm for 20 min. Oil-holding capacity was calculated as follows:

$$\text{Oil-holding capacity (g/g)} = (M_1 - M_2) / M_2$$

where M_1 represents the weight of the residue containing oil (g), and M_2 represents the weight of the sample (g).

Water swelling capacity

One gram of OSDF sample (M_0) was transferred into a graduated cylinder (250 mL), then 100 mL of distilled water were added. The cylinder was stand for 24 h at room temperature. The initial volume and the volume after swelling were recorded. Water swelling capacity was

estimated by the following formula:

$$\text{Water swelling capacity (mL/g)} = (V_1\text{-}V_0)/M_0$$

where V_1 is the dietary fiber volume after swelling (mL); V_0 is the dietary fiber volume before swelling (mL); M_0 is the OSDF sample weight (g).

Cation exchange capacity

The cation exchange capacity of OSDF was detected according to the method of Ruperez and Saura Calixto (2001). Three grams of OSDF was dissolved in 300 mL of 0.01 mol/L hydrochloric acid for 12 h. The mixture (2 mL) were titrated with 0.1 M NaOH to pH 7.0 and recorded the consumption volume of NaOH solution. Cation exchange capacity was expressed as consumed volume of NaOH.

Glucose adsorption capacity

The glucose adsorption capacity of OSDF was determined based on the method described by Benítez et al. (2017). Five grams of OSDF sample was mixed with 1 L glucose solution (100 mmol), then incubated at 37 °C for 2 h with constant shaking at 120 rpm (THZ-300C, Shanghai Yiheng Scientific Instrument Co., Ltd., Shanghai, China). After the mixture was centrifuged at 4000 rpm for 20 min at room temperature, the glucose concentration of the supernatant was determined using the 3, 5-dinitrosalicylic acid colorimetric method. Glucose adsorption capacity (mg/g) was calculated by the following equation:

$$\text{Glucose adsorption capacity (mg/g)} = (C_1\text{-}C_2) \times V/m$$

where C_1 represents the initial concentration of the glucose solution (mg/mL); C_2 represents the concentration of the glucose solution after being absorbed by OSDF (mg/mL); V represents the volume of the supernatant (mL); m represents the weight of OSDF (g).

Nitrite adsorption capacity

One gram of OSDF was mixed with 20 mL of 20 μg/mL sodium nitrite solution, and adjusted to pH 2.0 with 6 M hydrochloric acid and pH 7.0 with 2 M sodium hydroxide for simulating the small intestine and stomach environments, respectively. The mixtures were incubated at 37 °C for 20 min with continuous magnetic stirring and centrifuged at 4800 rpm for 10 min. The supernatants were collected. The remaining nitrite ion in the supernatant was measured by using the naphthylenediamine hydrochloride according to the method proposed by Gan et al. (2020). The nitrite ion adsorption capacity of OSDF was calculated as the following formula:

$$\text{Nitrite ion adsorption capacity (μg/g)} = (C_1\text{-}C_2) \times V/m$$

where C_1 is the nitrite concentration in the solution before adsorption (μg/mL); C_2 is the nitrite concentration of sample solution after adsorption (μg/mL); m represents the weight of OSDF (g); V represents the volume of sample solution (mL).

Bifidobacterium proliferative capacity

Fifty milligrams of OSDF sample was dissolved with 10 mL of liquid medium and sterilized at 121 °C for 15 min. After cooling, the media were inoculated with 1 mL of bifidobacterium and cultivated in an anaerobic incubator (YQX-III, Shanghai Wan Rui Industrial Co. Ltd., China) with 10% H_2, 10% CO_2, and 80% N_2 at 37 °C for 24 h. Liquid medium without OSDF was described as the control group. The absorbance value was determined at 620 nm to estimate to proliferative capacity of bifidobacterium.

X-ray diffraction spectroscopy

The crystalline structure of the OSDF samples were performed on a multipurpose X-ray diffractometer (Philips, MPD, Netherlands) with copper radiation at 40 kV and an incident current of 40 mA. The samples were analyzed in the step-scan mode with the 2θ diffraction angle ranging from 10° to 40° with a step of 0.02°/ s.

Fourier transform infrared spectroscopy (FTIR)

FTIR spectroscopy was conducted to investigate irradiation-induced structural changes. one milligram of OSDF samples was grinded, and mixed with 100 mg of KBr powder under infrared irradiation, followed by pressing to pellets. FT-IR spectra of the native and irradiated OSDF samples were recorded on a Nicolet 470 FT-IR spectrophotometer (Thermo Scientific, Waltham, USA) and the spectra were obtained in the wavelength range of 4000–400 cm^{-1} with a resolution of 4 cm^{-1}.

Scanning electron microscopy

The microscopic appearance of OSDF samples were observed with a scanning electron microscope (JSM-6390LV, JEOL, Tokyo, Japan). The dried samples were mounted on a cylindrical microscope stub covered with a carbon strip and coated with a thin layer of gold (5 min, 2 mbar) before observing.

Statistical analyses

Each experiment was carried out in triplicate. Statistical analyses were performed by SPSS Version 22 software (SPSS Inc., IL, USA). Differences among samples were determined by one-way ANOVA. The data were expressed as the mean ± standard deviation using a significance level of $P < 0.05$.

Results and discussion

Extraction yield of OSDF

The extraction yields of OSDF from navel orange peel irradiated at different doses are shown in Fig. 1. Irradiation treatment significantly enhanced the OSDF extraction yield. The extraction yield of OSDF at 12 kGy was significantly higher than that of other samples ($p < 0.05$). At the irradiation dose of 12 kGy, the extraction yield of OSDF reached 12.74%, which increased by 212.3% compared to the native sample. The regulatory mechanism may derive from the increase of water-soluble components, water-soluble monosaccharides and glycans after irradiation.

The intermolecular and intramolecular hydrogen bonds played important roles in stabilizing polysaccharides chains. Gamma-

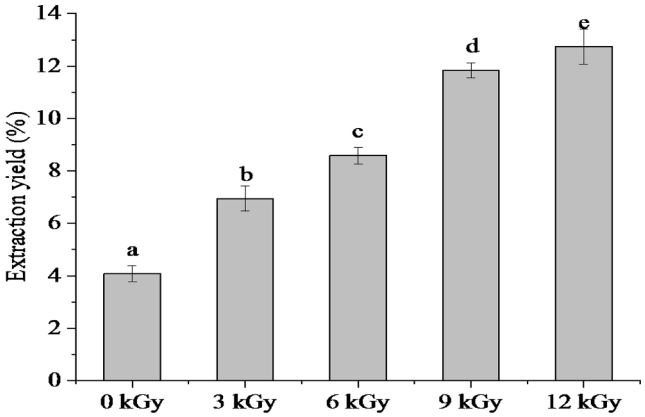

Fig. 1. The extraction yield of OSDF from navel orange peel irradiated at different doses. Data were expressed as means ± SD (n = 3) with different letters representing significant difference ($p < 0.05$).

irradiation affects these bonds and weakens van der Walls force (Sánchez Orozco et al., 2012). The increase of soluble dietary fiber content by irradiation has relation to the release of water-soluble carbohydrates in the transformation of insoluble dietary fiber (Fernandes et al., 2015). Previous research has reported the soluble dietary fiber content of soybean increases with the increasing irradiation dose from 400 kGy to 1200 kGy (Zhu et al., 2022). The result was similar to this research.

Monosaccharide composition

The monosaccharide composition of OSDF from navel orange peel irradiated with different doses are shown in Table 1. Rhamnose, arabinose, galactose, xylose, glucose, and galacturonic acid were detected. It is observed that glucose showed the highest content, followed by galactose and arabinose. After irradiation, the content of xylose, rhamnose, and arabinose was significantly reduced by 41.7%, 57.3%, and 54.7%, respectively. While the molar ratios of glucose and galacturonic acid showed an increasing trend by 43.3% and 11.6%. The dissociation and degradation extent of polysaccharides related to the irradiation dose.

Pectins are the most prevalent polysaccharides in citrus fibers (Lundberg et al., 2014), which are mainly composed of rhamnose, arabinose, galactose, xylose, glucose, and galacturonic acid (Wang et al., 2014). Due to the health benefit, gelling, thickening, and emulsification performances, pectins have been widely used in the food and pharmaceutical industries for several decades (Li et al., 2021). Glucose is mainly derived from cellulose and galacturonic acid is the main component of pectin, a characteristic polysaccharide of the cell wall (Zhang et al., 2018a). The changes in the monosaccharide composition related to the radiation intensity, which is possibly attributed to the breakage of glycosidic bond and the excessive degradation of the polysaccharide chain (Chen et al., 2021). In addition, the uronic acid content of the degraded samples was higher than that of the untreated polysaccharide due to degradation by irradiation, which leads to the further exposure of uronic acid in those unsoluble carbohydrates (Sánchez Orozco et al., 2012).

Molecular weight

Molecular weight can impact the hydration properties, cation exchange capacity, gel strength, texture, and application features of dietary fiber (Figuerola et al., 2005). High-performance gel permeation chromatography was applied to determine the molecular weight profile of OSDF at different irradiation doses. From Fig. 2, the fractions were eluted between 35 and 55 min with the molecular weight in the range of 126–545 kDa. Upon irradiation, there was a clear shift of retention time.

Table 1
The monosaccharide composition of OSDF from Navel orange peel irradiated at different dosages. The data are expressed as mean ± standard deviations (n = 3). Values mean in the same row followed by different superscript letters were significantly different ($p < 0.05$).

Monosaccharide (molar ratio)	Irradiation dose (kGy)				
	0	3	6	9	12
Rhamnose	0.012 ± 0.002^{b}	0.009 ± 0.001^{a}	0.009 ± 0.002^{a}	0.014 ± 0.001^{b}	0.007 ± 0.0^{a}
Arabinose	0.206 ± 0.006^{c}	0.189 ± 0.003^{b}	0.216 ± 0.009^{d}	0.074 ± 0.002^{a}	0.088 ± 0.002^{a}
Galactose	0.225 ± 0.003^{c}	0.187 ± 0.002^{b}	0.180 ± 0.003^{b}	0.096 ± 0.005^{a}	0.102 ± 0.003^{a}
glucose	0.402 ± 0.005^{a}	0.448 ± 0.009^{b}	0.424 ± 0.014^{b}	0.598 ± 0.011^{c}	0.576 ± 0.004^{d}
xylose	0.055 ± 0.003^{b}	0.045 ± 0.004^{a}	0.041 ± 0.001^{a}	–	–
Galacturonic acid	0.100 ± 0.004^{a}	0.122 ± 0.001^{b}	0.130 ± 0.002^{b}	0.202 ± 0.005^{c}	0.216 ± 0.003^{c}

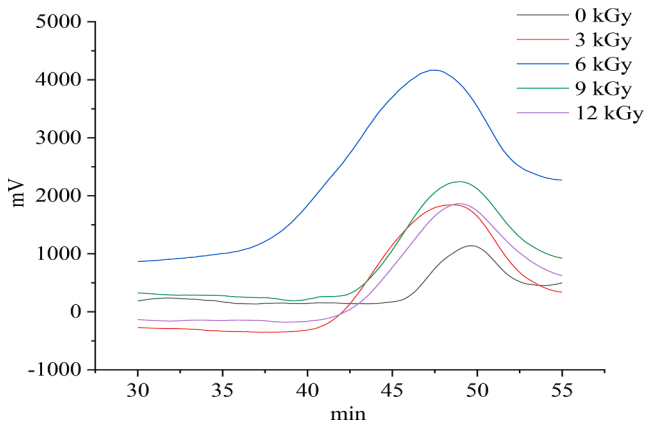

Fig. 2. The molecular weight distribution of OSDF from navel orange peel irradiated at different doses. Data were expressed as means ± SD (n = 3) with different letters representing significant difference ($p < 0.05$). (For interpretation of the references to color in this figure legend, the reader is referred to the web version of this article.)

The average molecular weight of the OSDF samples increased significantly ($p < 0.05$) with the irradiation dose of 0–6 kGy, thereafter decreased. At the irradiation dose of 9–12 kGy, the molecular weight of OSDF became stable and showed no obvious difference to the native OSDF sample.

Gamma irradiation is a low-energy and environmentally friendly sterilization technique in food production. However, high-dose irradiation can significantly destroy the structure of lignocellulose and increase the efficiency of enzymes (Zhu et al., 2022). Irradiation can influence the composition of OSDF in two aspects. One is the dissociation of depolymerization of insoluble polysaccharides into soluble polysaccharides. Another is the degradation of soluble polysaccharides into smaller polysaccharides, oligosaccharides, and monosaccharides (Ilyina et al., 2000). Furthermore, it results in the degradation of cellulose and increases the degradability of the cell wall constituents (Choi, Kim, & Lee, 2011). In general, the molecular weight of polysaccharides decreases proportional to the dosage of ionizing radiation. Li et al. (2011) have reported that low dose irradiation leads to an increased molecular weight, which is consistent with this research.

Physicochemical properties

Water holding capacity

Water holding capacity is an important feature of dietary fiber. It describes the maximum amount of absorbing and retaining water of dry material without being subjected to stress (Jeddou et al., 2016). The effect of irradiation doses on the water holding capacity of OSDF is presented in Fig. 3A. The water holding capacity of irradiated OSDF was significantly ($p < 0.05$) higher than that of the native sample, and reached the maximum values of 35.16 g/g at the irradiation dose of 6 kGy. Afterward, water holding capacity tended to decrease and presented a lower value at the irradiation dose of 12 kGy.

In general, water is held on the hydrophilic sites of the fiber itself or within void spaces in the molecular structure (Mudgil & Barak, 2013). With low dose irradiation, the water holding capacity of dietary fiber usually showed an increasing trend attributed to the breaking of glycosidic bonds and degradation of polysaccharides, which provided more space for the storage of water molecules. Besides, the structure feature such as a long side chain in arabinans and galactans can increase the hydrophilicity, which allows them to interact with the water in an unhindered way, resulting in a higher radius of gyration and hydrodynamic volume (Schmitz, Karlsson, & Adlercreutz, 2021). However, this trend was not dose-dependent. With the excessive radiation dose, the water holding capacity of fiber usually decreased due to the destruction

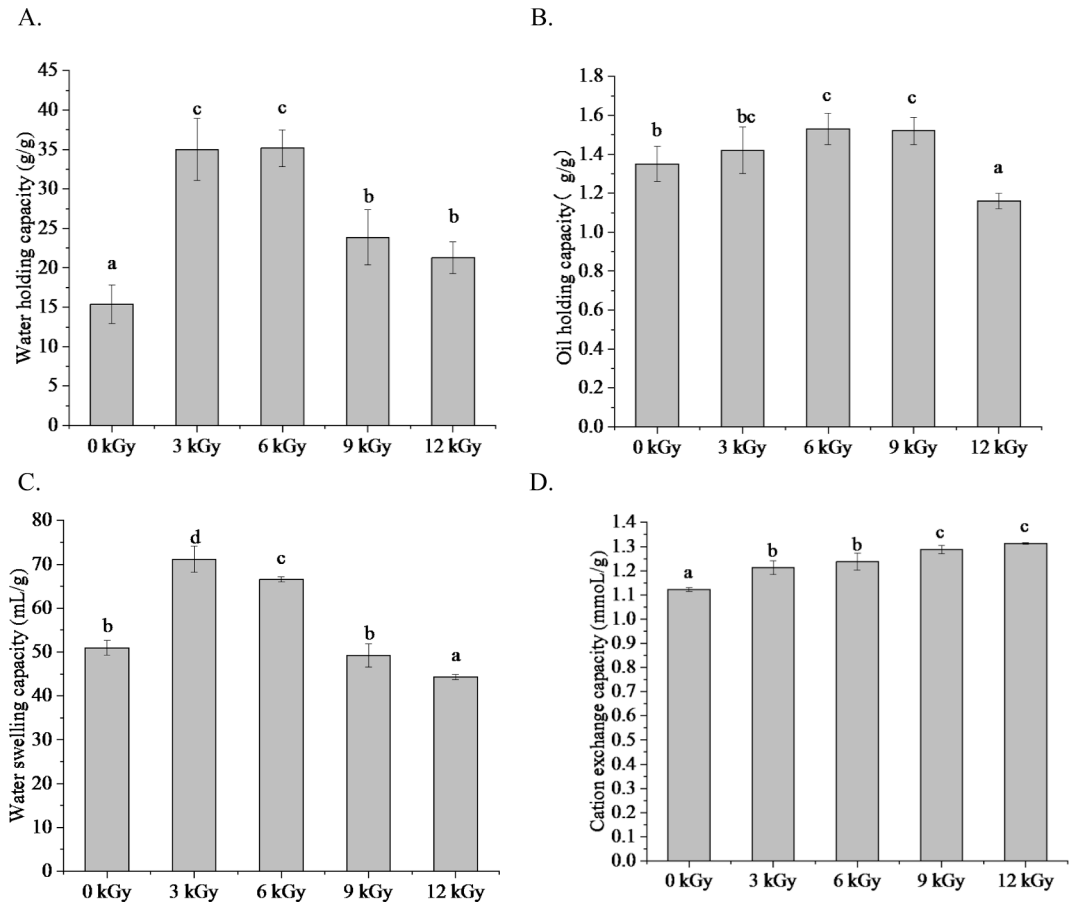

Fig. 3. Physiochemical properties of OSDF from navel orange peel irradiated at different doses. water holding capacity (A), oil holding capacity (B), water swelling capacity (C) and cation exchange capacity (D). Data were expressed as means ± SD (n = 3). Bars with different letters are significantly different ($p < 0.05$).

of the network structure.

Oil holding capacity

The oil holding capacity of OSDF plays an important role in food applications. It relates to the adsorption of organic compounds to the surface of the substrates, such as preventing fat loss during cooking or removing excess fat from the body. From Fig. 3B, the oil holding capacity of OSDF gradually increased and became relatively stable in the irradiation intensity of 6–9 kGy. Significant ($p < 0.05$) variations were observed in the oil holding capacity of the OSDF irradiated forms. After irradiation, the highest oil holding capacity of OSDF reached 1.53 g/g. This trend was similar to their water holding capacity change.

The oil holding capacity of dietary fiber is related to the chemical structure of polysaccharides, surface properties, electric charge density, and hydrophobicity of dietary fiber. The variation in the oil holding capacity of dietary fiber is attributed to the presence of hydrophobic regions that bind to the oil (Liu et al., 2021). Irradiation induced dissociation and degradation of polysaccharides, which further changed the steric structure in the oil/water system (Noguerol, Igual, & Pagán, 2022). In general, high water holding capacity and oil holding capacity suggest a good potential of dietary fiber applied in food products, which prevents moisture loss in formulated foods and serves as the emulsifier for high-fat foods.

Water swelling capacity

Water swelling capacity is a popular functional property in food processing. It is another indicator, in addition to water holding capacity, which is used to evaluate the hydration property of dietary fiber. As shown in Fig. 3C, there was a significant difference in the water swelling capacity of OSDF irradiated compared to the native sample ($p < 0.05$). The water swelling capacity did not show a linear relationship with the experimental irradiation range but an inverse U shape relationship. The maximum water swelling capacity of OSDF was 71.17 mL/g at the irradiation intensity of 3 kGy. Afterward, water swelling capacity decreased significantly ($p < 0.05$) with the irradiation dose increase, which is consistent with the water holding capacity change.

Water holding capacity and water swelling capacity are correlated with hydration properties and are important indicators for food functionality, preventing food from shrinkage. Dietary fiber can interact with water through two main mechanisms as surface tension strength and water held by hydrogen bonds and dipole forms (Huang et al., 2021). Hydroxyl group can form hydrogen bond with water molecules and contribute to improve the solubility in water. Moreover, Singh et al. (2011) have reported a reduced water swelling capacity of γ-irradiated potato starch, which is attributed to the loss in crystallinity.

Cation exchange capacity

A high cation exchange capacity of dietary fiber means the excellent properties for binding to heavy metals, like Hg, Pb, and Cd, which can remove ingested heavy metals and detoxify the human body (Zhang, Huang, & Ou, 2011). As shown in Fig. 3D, the cation exchange capacity of OSDF was in the range of 1.12–1.31 mmol/g within the irradiation dose of 0–12 kGy. The cation exchange capacity of OSDF irradiated at 9 or 12 kGy showed higher values than that of other irradiation doses ($p < 0.05$).

The cation exchange capacity of fiber depends on the presence of functional groups responsible for the exchange ability. These main functional groups related to the property include phenol hydroxyl group and carboxyl group from uronic acids in fibers. They produce a function similar to weak acidic cation exchange resin and reversibly interact with

cations (Chu et al., 2019). The higher cation exchange capacity of fibers is mainly due to the accumulation of soluble pectins and cleavage of carboxyl methyl ester into a carboxylic acid. After irradiation, the partial degradation of the fiber and the exposure of side groups such as hydroxyl and carboxyl helped to increase cation exchange capacity (Huang et al., 2021).

Glucose adsorption capacity

The glucose adsorption capacity index indicates the ability of dietary fiber to control postprandial blood glucose. It presented a vital functional property for dietary fibers. As shown in Fig. 4A, there was a significant difference among different irradiated samples ($p < 0.05$). After irradiation, the glucose adsorption capacity of OSDF was increased and reached a maximum value at the irradiation dose of 12 kGy, which values increased nearly twice compared to that of native OSDF. The higher adsorption capacity of the samples may be attributed to their dietary fiber content and the increase of cavities or spaces on the surface of the dietary fiber.

The ability of OSDF to adsorb glucose is beneficial to the reduced amount of glucose in the small intestine. Lopez et al. (2022) have reported that higher glucose adsorption capacity may attribute to the retention of glucose within the fiber network and reduction of water mobility on the fiber surface, as the hydration capacity of large particles increases, which may bind the glucose on the fiber surface. The exposure of polar and nonpolar groups enhances the interaction between dietary fiber and glucose molecules, as affected by the type and number of side-chain groups exposed under different irradiation (Saikia & Mahanta, 2016).

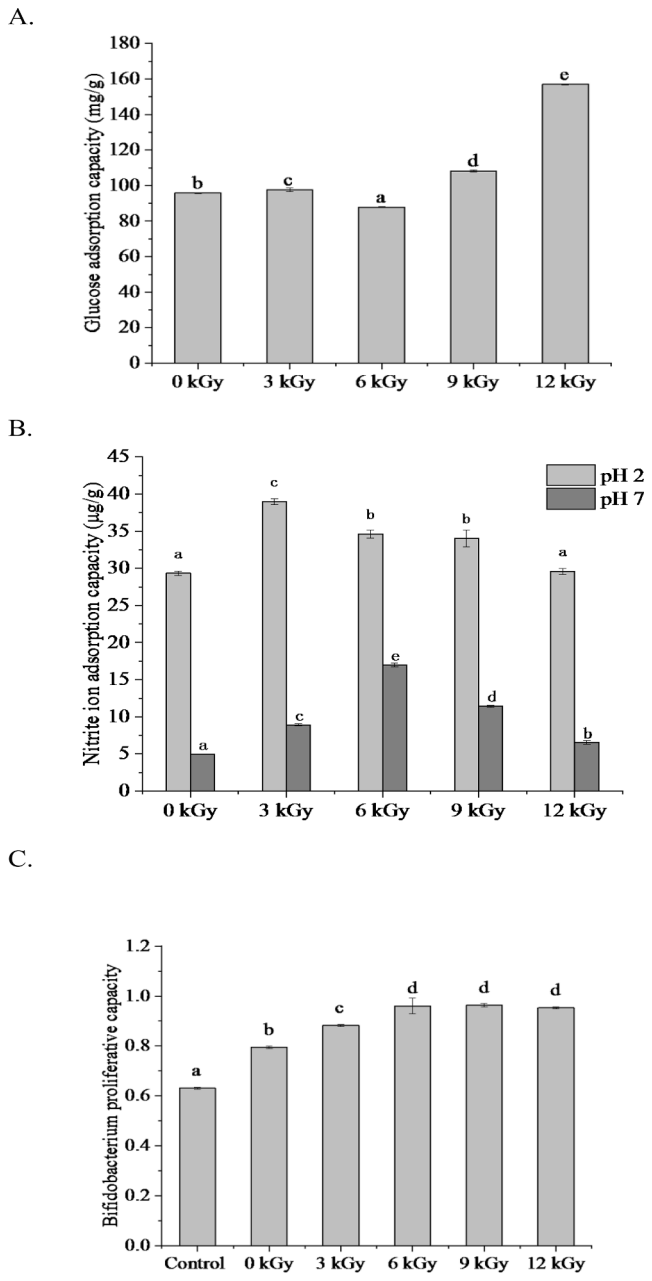

Fig. 4. Functional properties of OSDF from navel orange peel irradiated at different doses. Glucose adsorption capacity (A), nitrite ion adsorption capacity (B), and proliferation of bifidobacterium (C). Data were expressed as means ± SD (n = 3). Bars with different letters are significantly different ($p < 0.05$).

Nitrite adsorption capacity

Nitrosamine is recognized as a typical chemical carcinogen, which is synthesized from nitrite and secondary amine (Quist et al., 2018). The nitrite adsorption capacity of OSDF from navel orange peel irradiated at different doses are shown in Fig. 4B. In the simulated gastric environment (PH = 2), the nitrite adsorption capacity of irradiated OSDF (3–9 kGy) was significantly higher than that of native OSDF ($p < 0.05$). The maximum nitrite adsorption capacity of irradiated OSDF was 38.99 μg/g at 3 kGy, increased by 34.4%. In the simulated intestinal environment (pH = 7.0), compared to the native OSDF, a significantly higher nitrite adsorption capacity could be observed. There was a significant difference ($p < 0.05$) among different groups, and the maximum nitrite adsorption capacity values of OSDF was 16.97 μg/g at 6 kGy, increased by 240%. It was valuable mentioning that pH had an obvious effect on the nitrite adsorption capacity of OSDF, and the irradiated OSDF sample presented good effects in the stomach and intestine.

Under the gastric acid environment, nitrite reaction can induce the risk of cancer and cause fetal malformations. Active acid groups, especially uronic acid and phenolic acid, were the main contributors to nitrogen adsorption (Zheng et al., 2022). In acidic condition, NO^{2-} can combine with H^{+} to produce HNO_2 and further to form nitrogen–oxygen compounds such as N_2O_3. These compounds can bind to the negatively charged oxygen atoms of active acid groups in dietary fiber and cause adsorption (Lyu et al., 2021). The property of high nitrite ion adsorption capacity provides dietary fiber with the potential to be used as a functional food in protecting from gastric cancer development.

Bifidobacterium proliferation capacity

Bifidobacterium was a typical probiotic. It plays an important role in reducing intestinal LPS and fortifying intestinal barrier function (Reyed, 2007). The *bifidobacterium* proliferative capacity of OSDF from navel orange peel was measured after irradiation treatment at different doses (Fig. 4C). Different irradiated doses of OSDFs presented a significantly different effect ($p < 0.05$) on the proliferation of *bifidobacterium* compared to that of native OSDF. It was obvious to observe that the *bifidobacterium* proliferation capacity increased in a dose-dependent after irradiation and retained steady in the range of 6–12 kGy.

The health-promoting effects of prebiotic substrates are usually ascribed to the induction of the growth of the beneficial bacterial species and the production of short-chain fatty acids (Ashaolu, Ashaolu, & Adeyeye, 2021). Dietary fibers are the main source of nutrients for gut microbiota, which can modulate and improve microbial composition. The increase of proliferative capacity of *bifidobacterium* was mainly due to oligomeric saccharides content and the degree of polymerization. The low molecular weight polysaccharides degraded by gamma irradiation is one of the effective approaches for enhancing biological activities (Byun et al., 2008).

X-ray diffraction pattern

X-ray diffraction was applied to further evaluate changes in crystallinity and thus determine the aggregation state of the SDF molecules. The characteristic sharp diffraction reflects the crystalline structure, and the diffusion diffraction reflects the amorphous structure. The X-ray diffraction patterns of OSDF from navel orange peel irradiated at different doses are shown in Fig. 5A. The OSDF samples revealed the characteristic crystalline peaks at $2\theta = 15.8°$,19.6°, and 21.6°, whereas the prominent diffraction peak was around 21.6°, attributed to the cellulose I crystal structure, which was consistent with the structural characteristics of dietary fiber from lemon, orange and grapefruit seeds (Karaman, Yılmaz, & Tuncel, 2017). After irradiation, the characteristic peaks of OSDF were relatively gentle, and there was no obvious crystallization peak at 15.8° and 19.6°. The crystallinity values of OSDF were in the range of 39.46–41.15% within the irradiation dose of 0–12 kGy. Crystallinity value of OSDF irradiated at 12 kGy was slightly higher than those at other irradiation doses, but the difference was not significant ($p > 0.05$). The increase of crystallinity was mainly attributed to the cleavage of hydrogen bonds between cellulose and impairment of amorphous cellulose and part of crystalline cellulose. In addition, partial large crystals could be reconstructed during the processing after being destroyed into small crystals, increasing crystallinity.

FT-IR analysis

FTIR spectra of the modified fibers in the 400–4000 cm^{-1} regions were analyzed and the structural features of polysaccharides, such as glycosidic bonds, monosaccharides, and functional groups were attributed. As shown in Fig. 5B, the broad and intense characteristic absorption peak of OSDF with different radiation dosages at 3418 cm^{-1} were assigned to vibration of O—H groups, indicating the combination of hydrogen and the hydroxyl groups in cellulose and hemicelluloses. Changes in intensity were observed at several characteristic bands, confirming the impact of different irradiation treatments on the structure of OSDF. It seems similar with the degradation trend of cellulose or

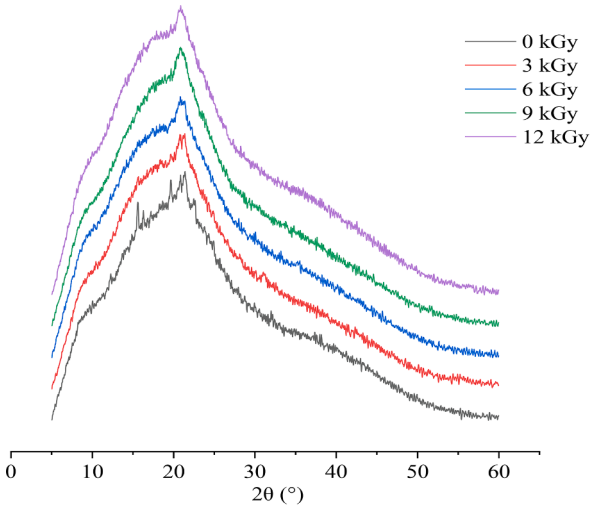

A

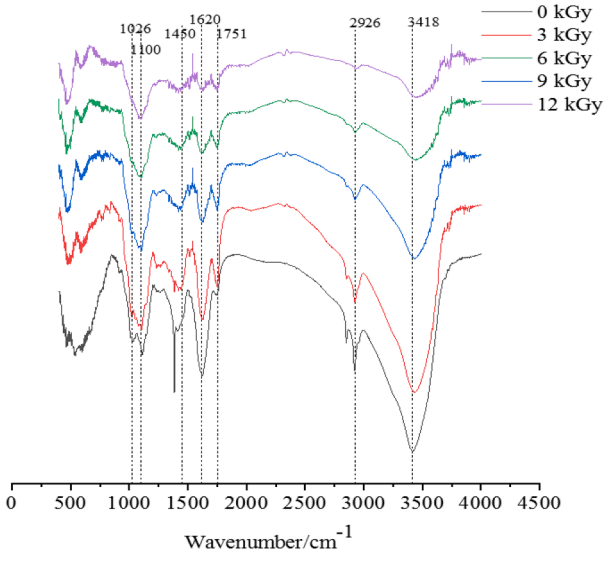

B

Fig. 5. X-ray diffratogram, FTIR spectra and microstructure of OSDF from navel orange peel irradiated at different doses. A, X-ray diffractogram; B, FTIR spectra; C, SEM graph of unirradiated OSDF; D, SEM graph of irradiated OSDF (3 kGy); E, SEM graph of irradiated OSDF (6 kGy); F, SEM graph of irradiated OSDF (9 kGy); G, SEM graph of irradiated OSDF (12 kGy). (For interpretation of the references to color in this figure legend, the reader is referred to the web version of this article.)

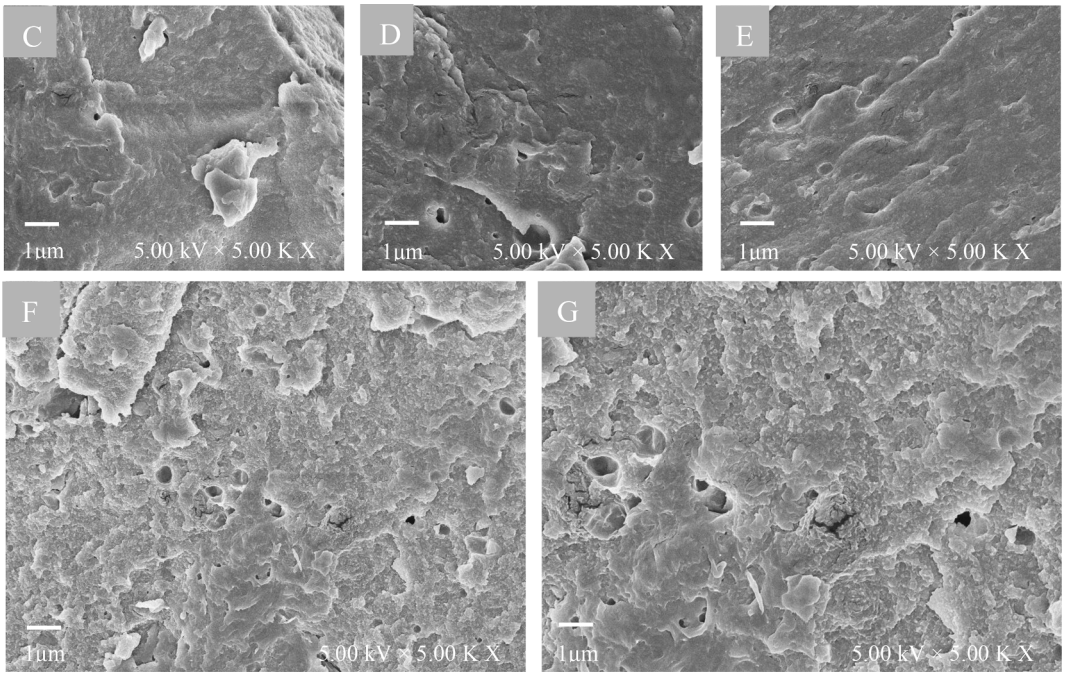

Fig. 5. (*continued*).

hemicellulose that the changing trend of intensity at some characteristic bands. The broad peak appearing at 2920–2935 cm^{-1} was the stretching vibration of the C—H bond, which was a characteristic absorption peak of the polysaccharide methyl and methylene groups (Gu et al., 2020).

A difference was observed in the height and shape of certain absorption bands at 1639 cm, which was associated with the formation of a carbonyl group. The change in spectra also confirmed that a carboxyl group was formed and that COO^- was interrupted during irradiation degradation of OSDF. Huang et al. (2007) have reported the formation of carboxyl or carbonyl groups in carboxymethylated chitosan following gamma irradiation. The absorption at 1415 cm^{-1} corresponded to bending vibration of C—H groups which were probably evoked by $–CH_2–$ bond types. The bands at 1736 and 1514 cm^{-1} were assigned to characteristic bending or stretching vibrations of the different groups from cellulose and lignin. The absorption peak at 1620 cm^{-1} was related to the C═C stretching vibration in alkenes, and the peak at 1016 to 1026 cm^{-1} was related to the C—O stretching vibration on the ester group.

The peak intensities of irradiated OSDF were generally weaker than the unirradiated OSDF samples. This phenomenon characterizes reduced hydrogen bonds in the linked state of OSDF, derived mainly from pectin (galacturonic acid) and hemicellulose (xylose, mannose, galactose, and arabinose), indicating that pectin and hemicellulose undergo partial degradation under irradiation conditions. It was noted that the absorption band observed at 881 cm^{-1} was assigned to β-glycosidic bond of OSDF, and the absorption band at 779 cm^{-1} was derived from stretching of C—O—C in α-pyranose ring. These peaks of modified OSDF reduced or disappeared, suggesting that the irradiation treatment could cause the reduction of hydrogen bonds in citrus fiber and lose its inner and surface structure (Mealer et al., 2012).

Microstructure

The images of the microstructure of OSDF from navel orange peel irradiated at different doses are presented in Fig. 5. The irradiated OSDFs showed a looser inner structure and exposed more microfibrils with increased treatment intensity compared to native OSDF. The surface of OSDF ruptured and appeared massive structure and holes in the range of 3–12 kGy. With the increase of irradiation dose, the number of pores increased and the microstructure was more fragmentary. However, when the radiation doses were 9 kGy and 12 kGy, the surface structure of OSDF was broken, the degree of polymerization decreased and the pores became larger. Irradiation might destroy the dietary fiber particle, which was consistent with the decrease of water swelling capacity and water holding capacity.

Previous studies exhibited irradiation treatment can efficiently degrade the cellulose and hemicellulose of the soybean fiber, leading to more significant cracks on the surface of the fiber. The greater ratio of lignins and cellulose are degraded by the pretreatment, the more porosity presents on the fiber surface. Cellulose and hemicellulose degradation can promote the formation of a honeycomb structure with more cracks on the surface. A larger surface and internal area of properly treated OSDF enabled a larger amount of water and oil molecules. The distinctive changes in the external and internal structures of OSDFs could affect the physicochemical properties of fibers.

Conclusions

Results obtained in our study showed the differences in the chemical structure, physicochemical properties and functions of the OSDF from navel orange peel modified by γ-irradiation treatment. Irradiation modification contributed to enhance significantly the content of OSDF from navel orange peel with a dose-dependent effect. With the increase of irradiation dose, the molar ratio of glucose and galacturonic acid increased by 43.3% and 11.6%, and rhamnose, arabinose and galactose decreased by 41.7%, 57.3% and 54.7%, respectively. The OSDF from navel orange peel irradiated at 3~6 kGy exhibited improved physicochemical features, including stronger water holding capacity, water swelling capacity, oil holding capacity and cation exchange capacity values, and enhanced functions of glucose adsorption capacity, nitrite ion adsorption capacity and bifidobacterium proliferative capacity. XRD, FTIR and SEM results indicated that irradiation could change the fibre crystalline regions. Increasing irradiation dose caused degradation of the dietary fiber structure, disruption of the crystallization area, broken covalent bonds, and loosen fiber structure. Therefore, γ-irradiation was an effective technique for preparation of modified OSDF from navel orange peel.

Declaration of Competing Interest

The authors declare that they have no known competing financial interests or personal relationships that could have appeared to influence the work reported in this paper.

Acknowledgments

The work was financially supported by Guangdong Provincial Key Research and Development Program of China (No. 2020B020226010), Guangdong Graduate Innovation and Entrepreneurship Training Program (No. 2017QTLXXM24) and Guangdong Provincial Key Laboratory of Lingnan Specialty Food Science and Technology (No. 2021B1212040013).

References

Ashaolu, T. J., Ashaolu, J. O., & Adeyeye, S. A. (2021). Fermentation of prebiotics by human colonic microbiota in vitro and short-chain fatty acids production: A critical review. *Journal of Applied Microbiology, 130*, 677–687.

Benítez, V., Mollá, E., Martín Cabrejas, M. A., Aguilera, Y., & Esteban, R. M. (2017). Physicochemical properties and in vitro antidiabetic potential of fibre concentrates from onion by-products. *Journal of Functional Foods, 36*, 34–42.

Byun, E. H., Kim, J. H., Sung, N. Y., Choi, J. I., Lim, S. T., Kim, K. H., … Lee, J. W. (2008). Effects of gamma irradiation on the physical and structural properties of β-glucan. *Radiation Physics and Chemistry, 77*, 781–786.

Chen, J., Huang, H., Chen, Y., Xie, J., Song, Y., Chang, X., … Yu, Q. (2020). Effects of fermentation on the structural characteristics and in vitro binding capacity of soluble dietary fiber from tea residues. *Food Science and Technology, 131*, Article 109818.

Chen, X., Sun Waterhouse, D., Yao, W., Li, X., Zhao, M., & You, L. (2021). Free radical-mediated degradation of polysaccharides: Mechanism of free radical formation and degradation, influence factors and product properties. *Food Chemistry, 365*, Article 130524.

Choi, J. I., & Kim, H. J. (2013). Preparation of low molecular weight fucoidan by gamma-irradiation and its anticancer activity. *Carbohydrate Polymers, 97*, 358–362.

Chu, J., Zhao, H., Lu, Z., Lu, F., Bie, X., & Zhang, C. (2019). Improved physicochemical and functional properties of dietary fiber from millet bran fermented by Bacillus natto. *Food Chemistry, 294*, 79–86.

Fernandes, Â., Barreira, J. C., Antonio, A. L., Morales, P., Fernandez Ruiz, V., Martins, A., … Ferreira, I. C. (2015). Exquisite wild mushrooms as a source of dietary fiber: Analysis in electron-beam irradiated samples. *Food Science and Technology, 60*, 855–859.

Figuerola, F., Hurtado, M. a. L., Estévez, A. M. a., Chiffelle, I., & Asenjo, F. (2005). Fibre concentrates from apple pomace and citrus peel as potential fibre sources for food enrichment. *Food Chemistry, 91*, 395-401.

Fuller, S., Tapsell, L. C., & Beck, E. J. (2018). Creation of a fibre categories database to quantify different dietary fibres. *Journal of Food Composition and Analysis, 71*, 36–43.

Gan, J., Huang, Z., Yu, Q., Peng, G., Chen, Y., Xie, J., Nie, S., & Xie, M. (2020). Microwave assisted extraction with three modifications on structural and functional properties of soluble dietary fibers from grapefruit peel. *Food Hydrocolloids, 101*, Article 105549.

Gill, S. K., Rossi, M., Bajka, B., & Whelan, K. (2021). Dietary fibre in gastrointestinal health and disease. *Nature Reviews: Gastroenterology & Hepatology, 18*, 101–116.

Gu, M., Fang, H., Gao, Y., Su, T., Niu, Y., & Yu, L. L. (2020). Characterization of enzymatic modified soluble dietary fiber from tomato peels with high release of lycopene. *Food Hydrocolloids, 99*, Article 105321.

Huang, M., Zhao, X., Mao, Y., Chen, L., & Yang, H. (2021). Metabolite release and rheological properties of sponge cake after in vitro digestion and the influence of a flour replacer rich in dietary fibre. *Food Research International, 144*, Article 110355.

Ilyina, A., Tikhonov, V., Albulov, A., & Varlamov, V. (2000). Enzymic preparation of acid-free-water-soluble chitosan. *Process Biochemistry, 35*, 563–568.

Jeddou, K. B., Chaari, F., Maktouf, S., Nouri Ellouz, O., Helbert, C. B., & Ghorbel, R. E. (2016). Structural, functional, and antioxidant properties of water-soluble polysaccharides from potatoes peels. *Food Chemistry, 205*, 97–105.

Karaman, E., Yılmaz, E., & Tuncel, N. B. (2017). Physicochemical, microstructural and functional characterization of dietary fibers extracted from lemon, orange and grapefruit seeds press meals. *Bioactive Carbohydrates and Dietary Fibre, 11*, 9–17.

Li, T., Wang, L., Chen, Z., Li, C., Li, X., & Sun, D. (2020). Structural changes and enzymatic hydrolysis yield of rice bran fiber under electron beam irradiation. *Food and Bioproducts Processing, 122*, 62–71.

Li, Y., Ha, Y., Wang, F., & Li, Y. (2011). Effect of irradiation on the molecular weight and structure and rheological behaviour of xanthan gum. *Scientia Agricultura Sinica, 44*, 4454–4463.

Lundberg, B., Pan, X., White, A., Chau, H., & Hotchkiss, A. (2014). Rheology and composition of citrus fiber. *Journal of Food Engineering, 125*, 97–104.

Li, D., Li, J., Dong, H., Li, X., Zhang, J., Ramaswamy, S., & Xu, F. (2021). Pectin in biomedical and drug delivery applications: A review. *International Journal of Biological Macromolecules, 185*, 49–65.

Liu, Y., Zhang, H., Yi, C., Quan, K., & Lin, B. (2021). Chemical composition, structure, physicochemical and functional properties of rice bran dietary fiber modified by cellulase treatment. *Food Chemistry, 342*, Article 128352.

Lyu, B., Wang, H., Swallah, M. S., Fu, H., Shen, Y., Guo, Z., … Jiang, L. (2021). Structure, properties and potential bioactivities of high-purity insoluble fibre from soybean dregs (Okara). *Food Chemistry, 364*, Article 130402.

Mealer, M., Jones, J., Newman, J., McFann, K. K., Rothbaum, B., & Moss, M. (2012). The presence of resilience is associated with a healthier psychological profile in intensive care unit (ICU) nurses: Results of a national survey. *International Journal of Nursing Studies, 49*, 292–299.

Min, Z., Gao, L., Gao, Y., Xu, C., Deng, X., & Xiao, Z. (2018). Optimization of the preparation process for soluble dietary fiber from rice bran by *Aspergillus niger* fermentation and its physicochemical properties. *Food Science, 39*, 112–118.

Mudgil, D., & Barak, S. (2013). Composition, properties and health benefits of indigestible carbohydrate polymers as dietary fiber: A review. *International Journal of Biological Macromolecules, 61*, 1–6.

Noguerol, A. T., Igual, M. M., & Pagán, M. J. (2022). Developing psyllium fibre gel-based foods: Physicochemical, nutritional, optical and mechanical properties. *Food Hydrocolloids, 122*, Article 107108.

Quist, A. J., Inoue-Choi, M., Weyer, P. J., Anderson, K. E., Cantor, K. P., Krasner, S., … Jones, R. R. (2018). Ingested nitrate and nitrite, disinfection by-products, and pancreatic cancer risk in postmenopausal women. *International Journal of Cancer, 142*, 251–261.

Reyed, M. (2007). The role of bifidobacteria in health. *Journal of Research in Medical Sciences., 2*, 14–24.

Rouhou, M. C., Abdelmoumen, S., Thomas, S., Attia, H., & Ghorbel, D. (2018). Use of green chemistry methods in the extraction of dietary fibers from cactus rackets (*Opuntia ficus indica*): Structural and microstructural studies. *International Journal of Biological Macromolecules, 116*, 901–910.

Ruperez, P., & Saura Calixto, F. (2001). Dietary fibre and physicochemical properties of edible Spanish seaweeds. *European Food Research and Technology, 212*, 349–354.

Saikia, S., & Mahanta, C. L. (2016). In vitro physicochemical, phytochemical and functional properties of fiber rich fractions derived from by-products of six fruits. *Journal of Food Science and Technology, 53*, 1496–1504.

Schmitz, E., Karlsson, E. N., & Adlercreutz, P. (2021). Altering the water holding capacity of potato pulp via structural modifications of the pectic polysaccharides. *Carbohydrate Polymer Technologies and Applications, 2*, Article 100153.

Sheng, Z., Liu, J., & Yang, B. (2021). Structure differences of water soluble polysaccharides in *Astragalus membranaceus* induced by origin and their bioactivity. *Foods, 10*, 1755.

Shridhar, K., Satija, A., Dhillon, P. K., Agrawal, S., Gupta, R., Bowen, L., … Reddy, K. S. (2018). Association between empirically derived dietary patterns with blood lipids, fasting blood glucose and blood pressure in adults-the India migration study. *Nutrition Journal, 17*, 1–12.

Singh, S., Singh, N., Ezekiel, R., & Kaur, A. (2011). Effects of gamma-irradiation on the morphological, structural, thermal and rheological properties of potato starches. *Carbohydrate Polymers, 83*, 1521–1528.

Sang, J., Li, L., Wen, J., Gu, Q., Wu, J., Yu, Y., … Lin, X. (2021). Evaluation of the structural, physicochemical and functional properties of dietary fiber extracted from newhall navel orange by-products. *Foods, 10*, 2772.

Threapleton, D. E., Greenwood, D. C., Evans, C. E., Cleghorn, C. L., Nykjaer, C., Woodhead, C., … Burley, V. J. (2013). Dietary fibre intake and risk of cardiovascular disease: Systematic review and meta-analysis. *British Medical Journal, 347*.

Wen, Y., Niu, M., Zhang, B., Zhao, S., & Xiong, S. (2017). Structural characteristics and functional properties of rice bran dietary fiber modified by enzymatic and enzyme-micronization treatments. *Food Science and Technology, 75*, 344–351.

Yang, D., Gao, S., & Yang, H. (2020). Effects of sucrose addition on the rheology and structure of iota-carrageenan. *Food Hydrocolloids, 99*, Article 105317.

Yang, J., Zeng, J., Wen, L., Zhu, H., Jiang, Y., John, A., … Yang, B. (2019). Effect of morin on the degradation of water-soluble polysaccharides in banana during softening. *Food Chemistry, 287*, 346–353.

Zhang, N., Huang, C., & Ou, S. (2011). In vitro binding capacities of three dietary fibers and their mixture for four toxic elements, cholesterol, and bile acid. *Journal of Hazardous Materials, 186*, 236–239.

Zheng, Y., Xu, B., Shi, P., Tian, H., Li, Y., Wang, X., … Liang, P. (2022). The influences of acetylation, hydroxypropylation, enzymatic hydrolysis and crosslinking on improved adsorption capacities and in vitro hypoglycemic properties of millet bran dietary fibre. *Food Chemistry, 368*, Article 130883.

Zhu, L., Yu, B., Chen, H., Yu, J., Yan, H., Luo, Y., … Mao, X. (2022). Comparisons of the micronization, steam explosion, and gamma irradiation treatment on chemical composition, structure, physicochemical properties, and *in vitro* digestibility of dietary fiber from soybean hulls. *Food Chemistry, 366*, Article 130618.

Further reading

Gorecka, D., Lampart Szczapa, E., Janitz, W., & Sokolowska, B. (2000). Composition of fractional and functional properties of dietary fiber of lupines (*L. luteus* and *L. albus*). *Nahrung, 44*, 229–232.